

the axis of maximum, is even more marked for NO_3^- . There is a 50 percent reduction in concentration at the southern edge of the data. There is also, as in the data for SO_4^{2-} concentrations, a large gradient along the coast.

The NH_4^+ data are not so neatly patterned. The lowest values, near 12 $\mu\text{mole/liter}$, extend from the Long Island site southwestward across Virginia to the West Virginia location. The highest NH_4^+ concentrations were measured over Ohio, Indiana, and Illinois with the maximum value for either network occurring at Champaign, Illinois (24 $\mu\text{mole/liter}$).

The pH pattern follows the general contours of the SO_4^{2-} and NO_3^- patterns. The north-south and coastal gradients are even sharper than for the individual ions since the H^+ concentrations combine the effects of both ions. The three highest H^+ values were 85, 82, and 82 $\mu\text{eq/liter}$ at Scranton, Pennsylvania; Ithaca, New York; and State College, Pennsylvania, respectively. These values represent pH values of 4.07 and 4.09 averaged over this 11-month period. The lowest H^+ concentrations were reported at the southern edge of the network at Raleigh, North Carolina, and Giles County, Tennessee, where both sites had an average H^+ concentration of 35 $\mu\text{eq/liter}$, which translates to a pH of 4.46.

These data show that precipitation chemistry data, carefully collected and rigidly quality-controlled, acquired by different organizations can be intermixed. This combination of data provides a much more comprehensive picture of the patterns than data from either network alone. The pattern analysis stops at the U.S. border since an attempt to incorporate Canadian precipitation chemistry data (11) for the same period of record and the same averaging technique indicated that those data did not compare to either the EPRI or MAP3S values.

For the first time in two decades, the United States has begun to produce a body of data that can be used to examine the chemistry of precipitation from individual storms as they pass across the eastern part of the country. These data will illuminate the nature of the variability in the chemistry (12). These results can be integrated and averaged to study the patterns and trends of anions and cations that control precipitation acidity. However, these data are only preliminary and this short period of record can tell little or nothing about trends in precipitation acidity or shifts in the proportional ion contributions to this acidity.

The sharp north-south gradients and the inability to locate the NH_4^+ maximum argue for the continuation of these existing networks and their extension south and west. The development of a National Plan for Acid Precipitation is under way. This analysis may be useful in establishing the monitoring aspects of the plan.

DONALD H. PACK

1826 Opalocka Drive,
McLean, Virginia 22101

References and Notes

1. G. E. Likens, R. F. Wright, J. N. Galloway, T. J. Butler, *Sci. Am.* **241** (No. 4), 43 (1979).
2. C. E. Junge and P. E. Gustafson, *Bull. Am. Meteorol. Soc.* **37**, 244 (1956).
3. J. P. Lodge, Jr., J. B. Pate, W. Basbergill, G. S. Swanson, K. C. Hill, E. Lorange, A. L. Lazrus, "Final report on the national precipitation sampling network" (National Center for Atmospheric Research, Boulder, Colo., 1968).
4. J. M. Miller, in *Proceedings of the World Meteorological Organization Technical Conference on Regional and Global Observations of Atmospheric Pollution Relative to Climate* (World Meteorological Organization, Geneva, in press).

5. M. T. Dana, "The MAP3S precipitation chemistry network: Second periodic summary report" (Battelle Pacific Northwest Laboratories, Richland, Wash., 1979).
 6. C. Hakkarinen, in *Proceedings: Advisory Workshop to Identify Research Needs on the Formation of Acid Precipitation* (Electric Power Research Institute, Palo Alto, Calif., 1979), p. S-2.
 7. J. W. Hornbeck, G. E. Likens, J. S. Eaton, *Water Air Soil Pollut.* **7**, 355 (1977); D. W. Pack, *Geophys. Res. Lett.* **5**, 673 (1978); D. H. Pack and D. W. Pack, in *Proceedings of the World Meteorological Organization Technical Conference on Regional and Global Observations of Atmospheric Pollution Relative to Climate* (World Meteorological Organization, Geneva, in press).
 8. M. E. Peden and L. M. Skowron, *Atmos. Environ.* **12**, 2343 (1978).
 9. M. T. Dana, personal communication. A forthcoming Battelle summary report will specify the fraction of data available at each site by season.
 10. C. D. Hodgman, Ed., *Standard Mathematical Tables* (Chemical Rubber, Cleveland, 1959), p. 253.
 11. *Canadian Network for Sampling Precipitation (CANSAP)* (Atmospheric Environment Service, Downsview, Ontario, 1979).
 12. The probability of various ion concentrations is now being investigated (D. H. Pack, in preparation).
 13. Support for this study was provided, in part, by the Environmental Assessment Department, Electric Power Research Institute.
- 6 February 1980; revised 27 March 1980

The Striking Resemblance of High-Resolution G-Banded Chromosomes of Man and Chimpanzee

Abstract. The fine structure and genetic organization of the chromosomes of man and chimpanzee are so similar that it is difficult to account for their phenotypic differences.

A comparative analysis of G-banded late prophase, prometaphase, and early metaphase chromosomes of humans and chimpanzees demonstrated that essentially every band and subband observed in man has a direct counterpart in the chimpanzee chromosome complement. The high-resolution technique employed allowed the observation of up to 1200 bands per haploid set, permitting the precise localization of breakpoints in the structural rearrangements that distinguish the two species. This work confirms and extends previous findings obtained with metaphase chromosomes (300 to 500 bands) that made it possible for earlier workers to agree in the 1975 report of the Paris Conference (1-3) that (i) human and chimpanzee chromosomes have a large degree of homology, (ii) the most conspicuous structural changes between the two species can be explained by a series of pericentric inversions and differences in amounts of centromeric and telomeric constitutive heterochromatin (4, 5), and (iii) the presence of 46 chromosomes in man and 48 in the chimpanzee can be explained by fusion of two acrocentric chromosomes to form the human chromosome 2. Because of the limited resolution of metaphase chromosomes, however, uncertainties persisted

as to the nature and extent of the observed structural differences. The fine detail achieved with the high-resolution G-banded chromosome technique developed in our laboratory (6) resolved such ambiguities because it was possible to follow, subband by subband, the virtually total homology that exists for non-heterochromatic bands in the two species.

Four female and two male chimpanzees (*Pan troglodytes*), as well as 7 adult women and 17 adult men, were examined. A detailed schematic representation of human G-banded chromosomes in late prophase, prometaphase, and early metaphase has been reported elsewhere (6) and was used as a standard for a detailed comparison between man and chimpanzee. To test for equivalence between chromosomes and bands in the two species, ten straight, sharply banded examples of each chromosome from both species were photographed at $\times 1600$ at each stage of chromosome condensation and enlarged approximately four times. The chromosomes of each stage were then matched side by side for a detailed analysis of banding patterns, band thickness, and staining intensity. To determine to what extent the banding patterns observed were related to het-

erochromatin, selected chromosome preparations were stained with the C-banding technique (7), which is known to preferentially stain constitutive heterochromatin. A description of similarities and differences in the two species was facilitated by arbitrarily ascribing the human high-resolution chromosome nomenclature (6) to chimpanzee chromosomes as well.

Figure 1 illustrates selected G-banded chromosomes of man and chimpanzee in

late prophase, prometaphase, and early metaphase. In addition, a schematic representation of all chromosomes in late prophase is illustrated in Fig. 2. In both figures, human and chimpanzee chromosomes are arranged to show maximum chromosome homology. The results illustrate the striking resemblance of the subbanding pattern of most chromosomes. For example, chromosome 3 is virtually identical in man and chimpanzee at various stages of chromosome

condensation (Fig. 1). Chromosomes 6, 8, 10, 11, 14, 19, 20, 21, 22, and X also have the same banding patterns and differ only in the addition of a telomeric G- and C-positive heterochromatic band (or bands) in the short or long arm of the corresponding chimpanzee chromosomes. Other chromosomes such as 1, 4, 5, 9, 12, 15, 16, 17, and 18 differ primarily in the presence of a pericentric inversion (Figs. 1 and 2). The remaining chromosomes (2, 7, 13, and Y) also have a very similar banding pattern in the two species but differ in specific features. Human chromosome 2 is generated by telomeric fusion (8) of two acrocentric chromosomes at the level of the upper two-thirds and lower one-third of band q13, followed by centromeric inactivation in one of the two chromosomes at the level of subband q21.2. Chromosomes 7 and 13 differ by the addition of G- and C-positive intercalated heterochromatin in the chimpanzee at the level of subbands 7q31.1 and 13q14.4. The Y chromosome of chimpanzee has a large amount of pericentromeric heterochromatin and a much smaller amount of heterochromatin in the distal end of the long arm, making this chromosome significantly smaller (Figs. 1 and 2). Other observed differences are the presence of a nucleolar organizer in the chimpanzee chromosome 18, with the corresponding feature found in the human chromosome 15 (Figs. 1 and 2), and the absence, or smaller amount, in chimpanzee of the constitutive heterochromatin that is close but not adjacent to the centromere (paracentromeric) in human chromosomes 1, 9, and 16.

With the use of high-resolution banded chromosomes it was possible to uncover information previously not attained. Perhaps the most important new finding is the striking homology of virtually all the nonheterochromatic subbands visualized in both species. Another important finding is the very precise localization of the observed structural differences, such as the fine localization of breakpoints in the pericentric inversions (Fig. 2) and the telomeric fusion of two acrocentric chromosomes to form human chromosome 2 (Figs. 1 and 2). Again, because of the fine detail obtained, two new pericentric inversions were found, a large one in chromosome 9 that probably passed unnoticed since this chromosome is not well banded in metaphase, and a very small inversion on chromosome 1 that can be clearly seen only in late prophase and prometaphases. Similarly, the telomeric heterochromatins on the short arm of chromosome 9 and on the

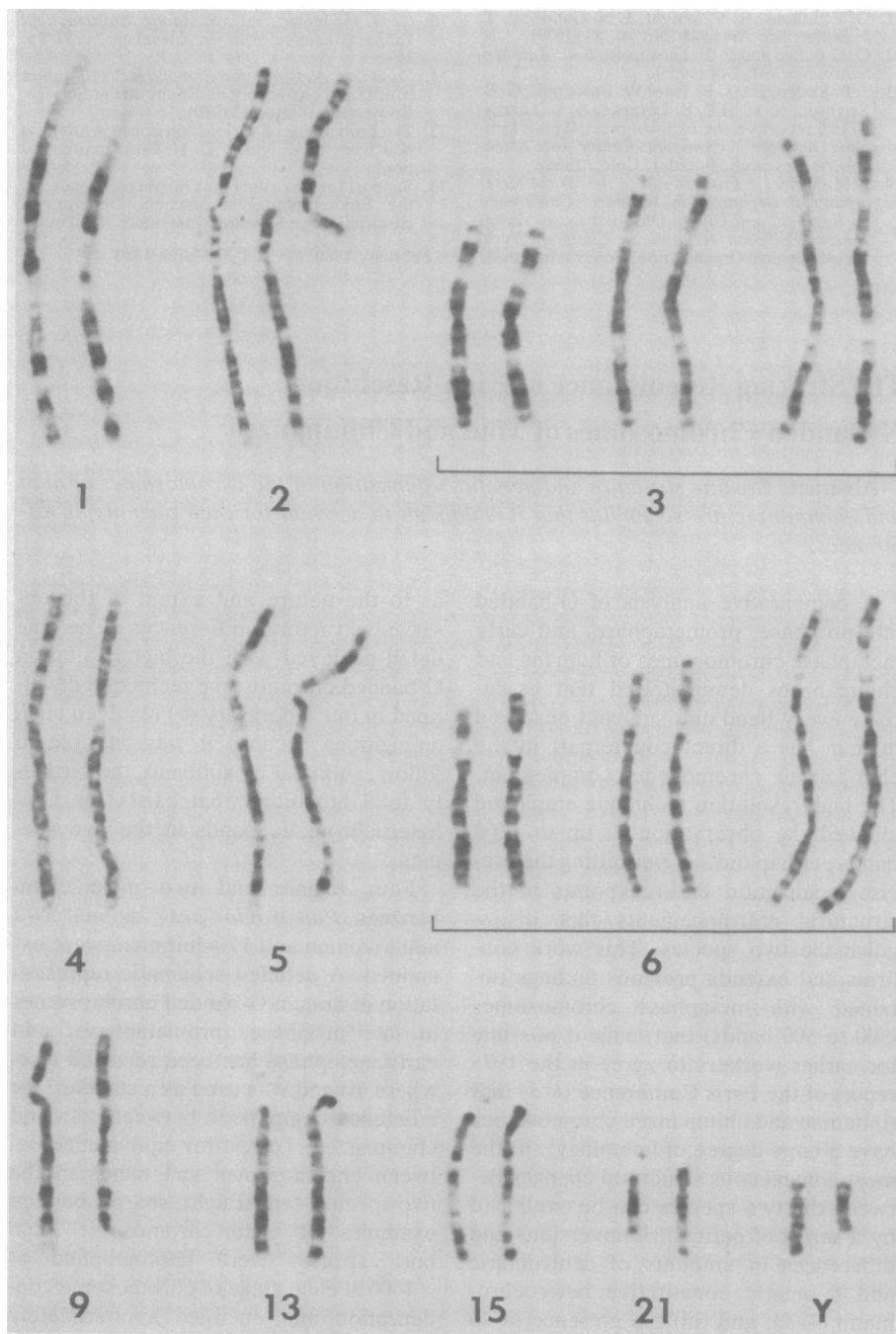


Fig. 1. Selected examples of Giemsa-banded chromosomes of man and chimpanzee arranged to show maximum homology with the human karyotype. The chromosomes of man are on the left and those of chimpanzee on the right. Chromosomes 3 and 6 are shown in early metaphase, prometaphase, and late prophase, respectively, to illustrate the homology that exists between chromosomes of these two species at various stages of chromosome condensation. Other selected chromosomes are shown in late prophase to illustrate structural differences and new findings.

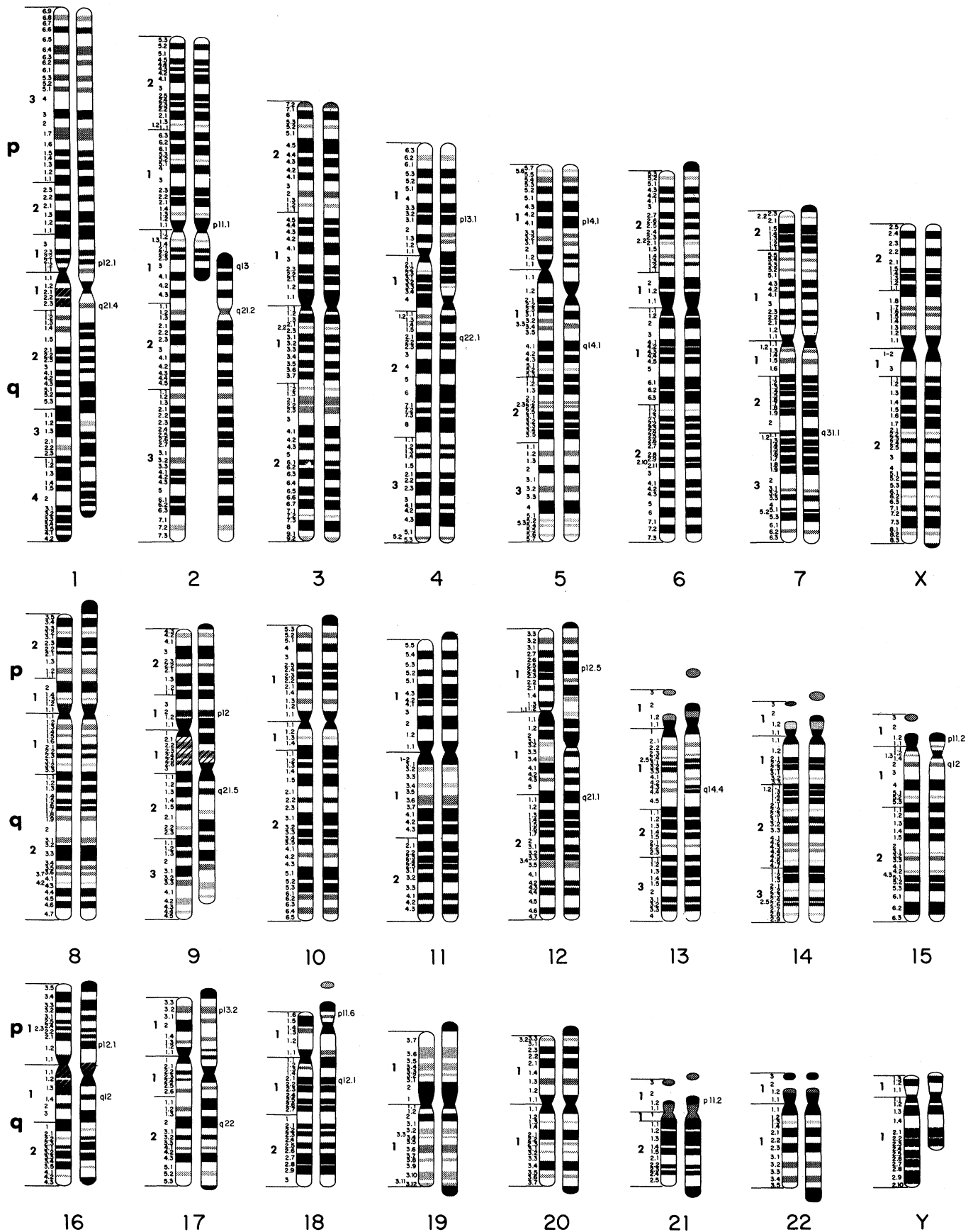


Fig. 2. Schematic representation of late prophase chromosomes of man and chimpanzee arranged to show maximum homology with the human chromosome complement. The chromosomes of man are shown on the left and those of chimpanzee on the right. The human chromosome nomenclature was used on the right of specific chimpanzee chromosome bands to facilitate a comparative analysis of breakpoints and structural differences. The schemes illustrate approximately 1000 bands. Paracentromeric and Y-type heterochromatin are represented with diagonals.

long arm of the X chromosome are so small that they can be detected only in late prophases (Fig. 2). Previously, the small chimpanzee Y chromosome was reported as indistinctly banded (1, 9). In this work, however, we found a banding pattern similar to that in man, except with less heterochromatin at the distal end of the long arm and more around the centromere (Figs. 1 and 2). Significant differences in the number and thickness of various bands on several chromosomes (4, 6, and 16) were shown in the comparative diagrams of the Paris report (3). These differences could not be confirmed in our detailed analysis of these chromosomes at various stages of condensation.

As a result of this and previous work, it has become evident that the chromosomal differences between man and chimpanzee are largely confined to the existence of nine pericentric inversions, addition of telomeric heterochromatin in 18 chimpanzee chromosomes (Fig. 2), and differences in amount of pericentromeric, paracentromeric, intercalated, and Y-type heterochromatin. The various types of constitutive heterochromatin are known to be enriched in nontranscribed highly repeated DNA sequences (5), and pericentric inversions have not been shown to produce changes in gene expression; therefore, the differences observed at the chromosomal level between man and chimpanzee appear to be of no consequence to their phenotype.

The virtual homology of the non-heterochromatic bands of man and chimpanzee is not surprising because more than 20 genes have been localized to homologous chromosomes and chromosome bands of the two species (10), the amino acid sequence of a large number of proteins studied in the two species is similar (11), and there is a large degree of homology of repeated and unique copy DNA in both species (12). Previous reports have also cited the finding of a chimpanzee with the clinical, behavioral, and cytogenetic features of Down's syndrome (13). Such a remarkable degree of similarity makes difficult a precise explanation of the large biological differences observed between these two closely related species.

JORGE J. YUNIS*

JEFFREY R. SAWYER

Department of Laboratory Medicine
and Pathology, University of Minnesota
Medical School, Minneapolis 55455

KELLY DUNHAM

Department of Preventive Medicine,
University of Iowa,
Oakdale 52319

References and Notes

1. C. C. Lin, B. Chiarelli, L. E. M. de Boer, M. M. Cohen, *J. Hum. Evol.* **2**, 311 (1973); J. de Grouchy, C. Turleau, M. Roubin, M. Klein, *Ann. Genet.* **15**, 79 (1972); P. Pearson, *Nobel Symp.* **23**, 145 (1973); J. Lejeune, B. Dutrillaux, M.-O. Rethoré, M. Prieur, *Chromosoma* **43**, 423 (1973).
2. B. Dutrillaux, "Sur la nature et l'origine des chromosomes humains," *Monogr. Ann. Genet. Expansion Sci. Fr.* (1975), pp. 41-71.
3. Paris Conference (1971), supplement (1975): "Standardization in human cytogenetics," *Cytogenet. Cell Genet.* **15**, 201 (1975).
4. A pericentric inversion represents an inversion of a chromosome segment that involves the centromere and has a breakpoint in each chromosome arm.
5. Constitutive heterochromatin represents chromosome material that is highly condensed in the interphase nucleus and is enriched in nontranscribed, highly repeated DNA sequences [J. J. Yunis and W. G. Yasmin, *Science* **174**, 1200 (1971); K. W. Jones, in *Molecular Structure of Human Chromosomes*, J. J. Yunis, Ed. (Academic Press, New York, 1977), p. 295].
6. J. J. Yunis, J. R. Sawyer, D. W. Ball, *Chromosoma* **67**, 293 (1978); J. J. Yunis, D. W. Ball, J. R. Sawyer, *Hum. Genet.* **49**, 291 (1979).
7. J. J. Yunis, L. Roldan, W. G. Yasmin, J. C. Lee, *Nature (London)* **231**, 532 (1971); M. E. Chandler and J. J. Yunis, *Cytogenet. Cell Genet.* **22**, 352 (1979).
8. Dutrillaux (2) considers the fusion as telomeric and interprets the terminal heterochromatin seen in the two chimpanzee acrocentric chromosomes to have arisen after the divergence of the two species.
9. D. A. Miller, *Science* **198**, 1116 (1977).
10. P. L. Pearson, in *Molecular Structure of Human Chromosomes*, J. J. Yunis, Ed. (Academic Press, New York, 1977), p. 267.
11. M.-C. King and A. C. Wilson, *Science* **188**, 107 (1975).
12. P. L. Deininger and C. W. Schmid, *ibid.* **194**, 846 (1976).
13. H. M. McClure, K. H. Belden, W. A. Pieper, C. B. Jacobson, *ibid.* **165**, 1010 (1969); F. H. Ruddle and R. P. Creagan, *Annu. Rev. Genet.* **9**, 407 (1975).
14. This research was supported by NIH grant GM26800 (to J.J.Y.).

* Correspondence should be addressed to J.J.Y.

3 December 1979

Oxygen Consumption and Cellular Ion Transport: Evidence for Adenosine Triphosphate to O₂ Ratio Near 6 in Intact Cell

Abstract. Oxygen (O₂) consumption and net K⁺ uptake were measured simultaneously upon reintroduction of K⁺ into a K⁺-depleted suspension of renal tubules. The K⁺/O₂ stoichiometries of 11.8 ± 0.2 and 8.4 ± 0.6 were obtained for reduced nicotinamide adenine dinucleotide- and flavoprotein-linked substrates, respectively. These values complement classical K⁺ to adenosine triphosphate (ATP) and ATP/O₂ stoichiometries, thereby demonstrating a remarkably efficient coupling between the processes of Na⁺- and K⁺-dependent adenosinetriphosphatase-mediated ion transport and oxidative phosphorylation within the intact cell.

Potassium uptake and sodium extrusion by mammalian epithelial cells are dependent on oxidative metabolism and Na⁺- and K⁺-dependent adenosinetriphosphatase (ATPase)-mediated ion transport. Individually, the production of adenosine triphosphate (ATP) by way of oxidative phosphorylation and the hydrolysis of ATP by the Na⁺,K⁺-ATPase have been well documented (1-3). However, the scheme by which these two fundamental processes work in concert

within the intact cell has not been entirely defined. Measurements of renal cell adenine nucleotide levels by Balaban *et al.* (4) lend experimental support to the contention (5) that the generation of adenosine diphosphate (ADP) by the Na⁺,K⁺-ATPase is instrumental in providing the signal for synchronous oxidative metabolism. These measurements suggest that the processes of transport and oxidative phosphorylation are coupled within the intact cell via their

Table 1. The K⁺/O₂ ratio for potassium uptake in K⁺-depleted renal tubules. The K⁺/O₂ ratios were calculated on the basis of individual experiments as illustrated in Fig. 1A. Average values for the absolute rates of QO₂ and K⁺ uptake are provided for the purposes of comparison between the substrates. Succinate-supplemented cells were prepared by using a modified K⁺-free suspension medium containing NaCl (100 mM), NaHCO₃ (25 mM), NaH₂PO₄ (4 mM), CaCl₂ (2.3 mM), MgSO₄ (2.0 mM), Na₂-succinate (20 mM), glucose (5 mM), and dextran (molecular weight, 40,000; 0.6 percent). The temperature was 37°C and the pH 7.4. Protein concentrations were in the range of 4 to 10 mg/ml. Values are given as means ± standard error.

Substrate	Experiments (No.)	K ⁺ /O ₂	QO ₂ (nmole O ₂ /min-mg protein)		K ⁺ uptake immediately after KCl addition (nmole K ⁺ /min-mg protein)
			Prior to KCl addition	KCl addition	
Glucose + lactate + alanine	16	11.8 ± 0.2	11 ± 1	20 ± 1	103 ± 7
Succinate + glucose	4	8.4 ± 0.6	29 ± 4	42 ± 6	112 ± 30